Check for updates

Synthesis, structures and magnetic properties of isoreticular polyrotaxane-type two-dimensional coordination polymers†

In-Hyeok Park, [ID] [ac] Tun Seng Herng, [ID] [bc] Huiyeong Ju, [ID] [a] Jun Ding, [ID] *[c]
Shim Sung Lee [ID] *[a] and Jagadese J. Vittal [ID] *[c]

Two isoreticular polyrotaxane-type two-dimensional coordination polymers (2D CPs) [Co$_2$(bpy)(sdb)$_2$]·2H$_2$O (**1**) and [Co$_2$(bpe)(sdb)$_2$]·DMA·1.5H$_2$O (**2**) (where sdb = 4,4′-sulfonyldibenzoate; bpy = 4,4′-bipyridyl and bpe = 4,4′-bipyridyl ethylene) have been synthesized and their solid state structures have been determined by X-ray crystallography. The solid state structures made up of wheels and axles have been synthesized using a bent dicarboxylate (sdb), two linear spacer ligands and Co(II). Interestingly, the sheets are two-fold entangled by [Co$_2$(sdb)$_2$Co$_2$] wheels and bpy or bpe axles. Due to the shorter length of the bpy ligand, the [Co$_2$(sdb)$_4$] moieties in **1** are brought closer than in the sheet formed in **2**. The magnetic properties of **1** and **2** have been discussed and fitted according to a spin Hamiltonian. **1** showed predominantly antiferromagnetic interactions with exchange integral of −1.522 cm^{-1}. While **2** exhibited the paramagnetic behaviour below 40 K and antiferromagnetic behaviour at higher temperature.

Introduction

Coordination polymers (CPs) are a class of highly crystalline materials formed by metal ions or metal clusters with exo-dentate spacer ligands.[1,2] One, two and three-dimensional CPs can be designed to exhibit high surface area, porosity, optical and magnetic properties.[3–7] Among these, polyrotaxane structures can be designed from wheels formed by two bent spacer ligands with two metal ions and axles from linear spacer co-ligands.[8–18] For instance, the two-dimensional (2D) CPs containing polyrotaxane structures can be designed and constructed from bent dipyridyl ligands and linear dicarboxylates or *vice versa*.[19–25] Recently, we reported several supramolecular isomers in polyrotaxane-type CPs of Zn(II) and Co(II) using a bent ligand, 4,4′-sulfonyldibenzoate (sdb, Scheme 1) and a long linear spacer ligand, 1,4-bis[2-(4′-pyridyl)ethenyl]benzene (bpeb).[26,27] The polyrotaxane-type Co(II) CPs show typically antiferromagnetic behaviour due to the long spacer ligand bpeb which prevents the neighbouring paddlewheel Co(II) coming closer in the solid state structures. Hence we have employed shorter bipyridyl spacer ligands namely 4,4′-bipyridyl (bpy) and

4,4′-bipyridyl ethylene (bpe) to synthesize similar polyrotaxane CPs and investigated their magnetic behaviour (Scheme 1). The details are given below.

Results and discussion

The single crystals of [Co$_2$(bpy)(sdb)$_2$]·2H$_2$O (**1**) and [Co$_2$(bpe)(sdb)$_2$]·DMA·1.5H$_2$O (**2**) were synthesized by the
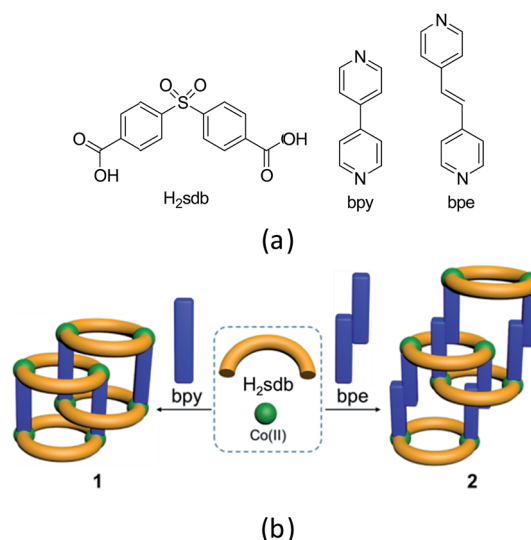
Scheme 1 (a) Structural diagrams of H$_2$sdb, bpy and bpe. (b) Polyrotaxane structures (**1** and **2**) formed from these two ligands with Co(II).

[a]Department of Chemistry and Research Institute of Natural Science, Gyeongsang National University, Jinju 52828, South Korea. E-mail: sslee@gnu.ac.kr

[b]Department of Materials Science and Engineering, National University of Singapore, 119260, Singapore. E-mail: msedingj@nus.edu.sg

[c]Department of Chemistry, National University of Singapore, 3 Science Drive 3, 117543, Singapore. E-mail: chmjjv@nus.edu.sg

solvothermal reactions of $Co(NO_3)_2 \cdot 6H_2O$ and H_2sdb with bpy or bpe, respectively, in the equimolar ratio in the mixtures of dimethylformamide (DMF) or dimethylacetamide (DMA)/dimethylsulfoxide (DMSO)/water at 120 °C. The two isoreticular polyrotaxane-type 2D CPs (1 and 2) are constructed from the paddlewheel repeating unit $[Co_2(O_2C–C)_4]$. The adjacent paddlewheel units are bridged by two sdb ligands to form a ring, $[Co_2(sdb)_2Co_2]$ thus generates a one-dimensional (1D) structure. These chains are further connected by the bpy or bpe spacer ligands in the axial positions of the paddlewheel units yielding 2D CPs. Interestingly, the $[Co_2(sdb)_2Co_2]$ rings and bpy (1) or bpe (2) axles from the neighbouring 2D structures produced polyrotaxane structures. The bulk homogeneity of the both products was confirmed by PXRD patterns (Fig. S1 and S2†). The details of the individual structures are described below.

$[Co_2(bpy)(sdb)_2] \cdot 2H_2O$ (1)

Blue blocks of single crystals of $[Co_2(bpy)(sdb)_2] \cdot 2H_2O$ (1) crystallized in orthorhombic space group $Cmcm$ with $Z = 4$ and the asymmetric unit contains quarter of the formula unit. In the crystal structure of 1 (Fig. 1), the atoms Co1, Co2, N1, C3, C4 and N2 have crystallographic $m2m$ symmetry and the other C atoms in the bpy ligand occupy crystallographic m plane. The paddlewheel is produced by applying this $m2m$ operation (Fig. 1a). Two sdb ligands are bonded to two neighbouring paddlewheels along a-axis forming $Co_2(sdb)_2$ ring (Fig. 1b). The Co–Co diagonal distance in this ring, 12.737 Å corresponds to the length

a of the unit cell. The axial positions are occupied by bpy ligands which are along the crystallographic b-axis. The distance of the Co–bpy–Co···Co repeating unit, 13.765 Å is the length b of unit cell. The connectivity of $Co_2(bpy)(sdb)_2$ produced a 2D structure in ab-plane with S1, O3 and O4 atoms sit on crystallographic m plane. Two-fold entanglement of these rings formed by $Co_2(sdb)_2$ with dimension, 8.59 Å × 8.59 Å (the distances between centres of Co(II) and S···S distances in the ring) by the axle bpy ligands from the neighbouring 2D structure generates a polyrotaxane structure (Fig. 1c–f). This polyrotaxane entanglement has been observed in several 2D structures before.[8–27] By virtue of X-ray crystallographic symmetry, bpy ligand is at the centre of this square cavity. The total potential solvent accessible area volume as calculated by PLATON in 1 is 288.3 Å³ which is 7.6% of the unit cell volume 3809.5 Å³ despite two-fold interpenetration.[28–30]

$[Co_2(bpe)(sdb)_2] \cdot DMA \cdot 1.5H_2O$ (2)

The dark violet block-shaped single crystals of $[Co_2(bpe)(sdb)_2] \cdot DMA \cdot 1.5H_2O$ (2) crystallized in monoclinic space group $P2_1/c$ with $Z = 4$. Similar to 1, the structure of 2 also adopts a doubly-entangled 2D structure (Fig. 2). The asymmetric unit contains a formula unit. The coordination mode at the Co(II) centre is square-pyramid with four oxygen atoms from four sdb ligands in the square-plane and one nitrogen atom of the bpe ligand at the apical position. The paddlewheel repeating units are connected to four sdb ligands and propagate along the c-axis via $Co_2(sdb)_2$ ring to form a 1D polymeric structure (Fig. 2a–c). The
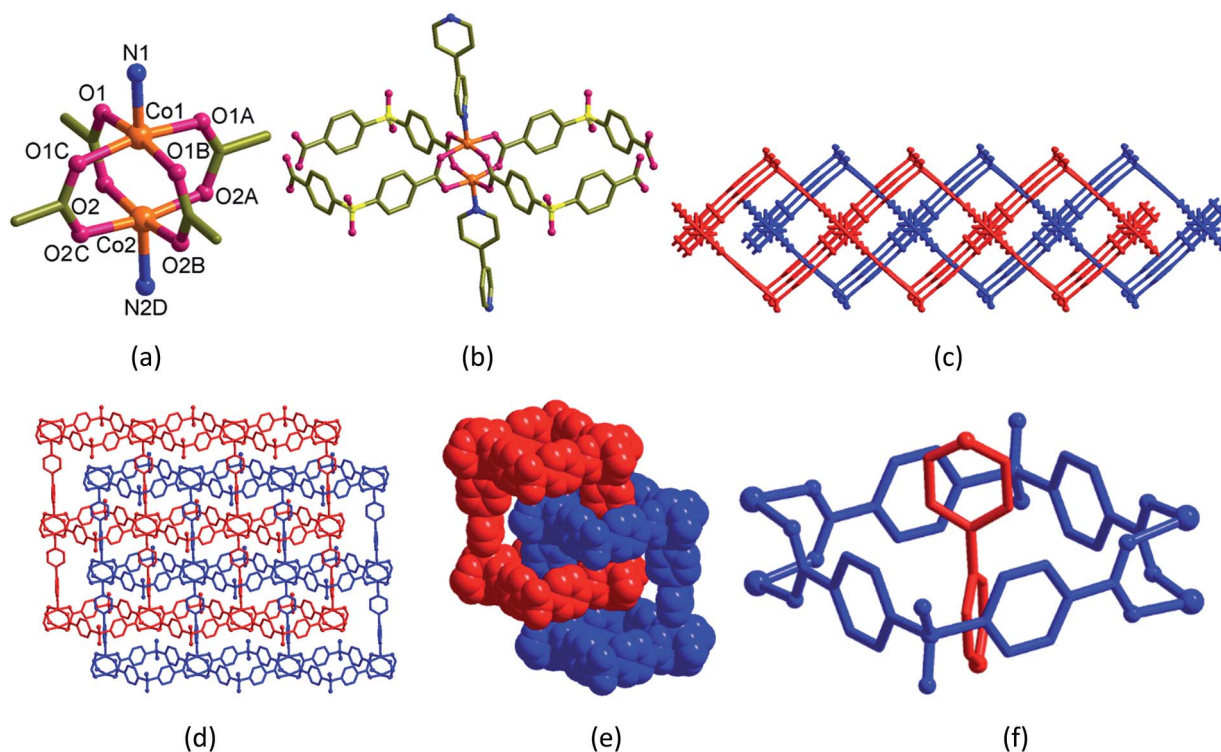

Fig. 1 2D grid-type polyrotaxane of $[Co_2(bpy)(sdb)_2] \cdot 2H_2O$ (1). (a) Coordination environment of Co(II) atoms. Symmetry codes: (A) $1 - x$, y, z; (B) $1 - x$, y, $1/2 - z$; (C) x, y, $1/2 - z$; (D) x, $-1 + y$, z. (b) Basic building unit. (c) Top view. (d) The 2-fold entanglement showing the 2D square-type grids. (e) and (f) Rotaxane units.
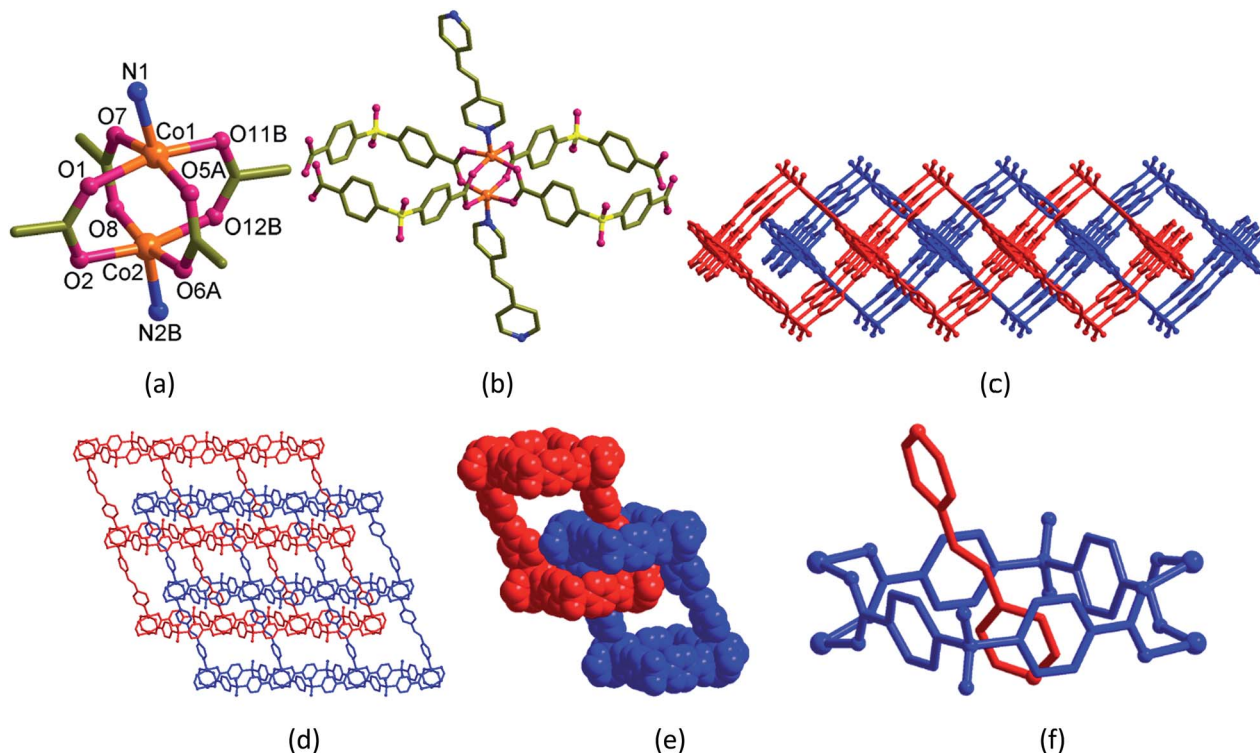
Fig. 2 2D polyrotaxane structure of $[Co_2(bpe)(sdb)_2] \cdot DMA \cdot 1.5H_2O$ (**2**). (a) A view showing the environment of Co(II) atoms. Symmetry codes: (A) $x, y, 1 + z$; (B) $x - 1, y, z$. (b) Basic building unit. (c) Top view. (d) The 2-fold entanglement of the 2D parallelogram grids. (e) and (f) Rotaxane units.

square cavity has dimension of 8.58 Å $\times$ 8.61 Å (the distances between centres of Co(II) and S···S distances in the ring) producing a 1D structure with square cavities due to the use of bent sdb ligand. The bpe ligand also acts as a pillar to this 1D structure to produce the layered structure (Fig. 2d) with crystallographic glide plane and inversion centre.

Like **1**, the linear bpe ligand also penetrates the $[Co_2(sdb)_2]$ square ring to form a rotaxane structure in the 2D grid of **2**. The pyridyl ring of bpe ligand is occupied in the cavity centre of the square ring. Again, the unusual entanglement of polyrotaxane was generated by rotaxane arrangement in **2**. The total potential solvent area volume as calculated by PLATON in **2** is 874.6 Å³ which is 20.2% of the unit cell volume 4327.7 Å³ despite two-fold interpenetration (Fig. 2d–f).[28–30] The void volume was partially occupied by one DMF and one and half water molecules. Unlike **1** showing a square-type grid (Fig. 1d), the 2D parallelogram grid in **2** (Fig. 2d) is generated from the distortion of the paddlewheel structure (Fig. 2a) and the longer length of the bpe spacer ligand.

Magnetic properties

As shown in Fig. 3, **1** and **2** display very contrast $\chi_m T$ behaviour. For **1**, $\chi_m T$ increases drastically from 0.27 cm³ K mol⁻¹ at 2 K to 3.08 cm³ K mol⁻¹ at 50 K. Above 50 K, $\chi_m T$ of these samples increases monotonically with increasing temperature. Such $\chi_m T$ reduction at low temperature may associate with the presence of antiferromagnetic exchange coupling between the Co(II) ions and/or to the depopulation of the higher energy

Kramers doublets of the Co(II) centres with a $4T1$ term as the ground state. At room temperature (300 K), **1** exhibits $\chi_m T$ value of 3.54 cm³ K mol⁻¹ that is higher than expected 1.87 cm³ K mol⁻¹ for spin only high spin Co(II) ions ($S = 3/2$ and $g = 2$) and it is closed to the theoretical value ($\sim$3.3 cm³ K mol⁻¹) of spin-orbital coupling of Co(II) ions. Thus, this phenomenon may be attributed to the spin-orbital coupling of Co(II) ions.

For **2**, the value of $\chi_m T$ remains nearly constant from 2 K up to 40 K, suggesting the paramagnetic behaviour. Then the $\chi_m T$ increases monotonically with increasing temperature with $\chi_m T$
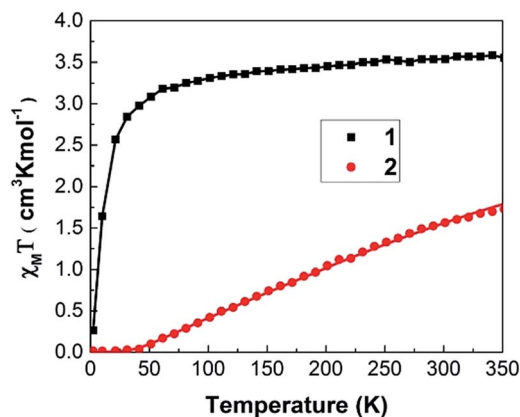

Fig. 3 Temperature dependence of $\chi_m T$ for **1** and **2** measured at 500 Oe from 2 to 350 K. The samples are fitted according to a spin Hamiltonian by the PHI program with $g = 1.91$ for **1** and 2.02 for **2** (solid lines).

of 1.56 cm^3 K mol^{-1} at 300 K. This phenomenon suggests the presence of antiferromagnetic exchange coupling in the CP with increasing temperature.[32,33] It is noted that the value of $\chi_m T$, 1.56 cm^3 K mol^{-1} at 300 K is same order of magnitude as the expected 1.87 cm^3 K mol^{-1} for spin only high spin Co(II) ions ($S = 3/2$ and $g = 2$). Thus, magnetic properties of **2** mainly predominated by high spin Co(II) ions.

The magnetic susceptibility data were fitted according to a spin Hamiltonian by the PHI[31] program with $g = 1.91$ for **1** and 2.02 for **2** in the temperature range of 2–350 K. The best fitted data yielded the exchange integral J of -1.522 cm^{-1} for **1** and -61.281 cm^{-1} for **2** respectively. Both samples exhibit a temperature independent paramagnetic (TIP) component of 5.0×10^{-4} cm^3 K mol^{-1}. These results indicate that antiferromagnetic interaction exists within the Co(II) dimer unit[31,32] **1** and **2** shows axial zero field splitting (ZFS) parameter (D) of 4.69 and 4.49 cm^{-1}, respectively, with the rhombic ZFS parameter (E) of ± 0.056 cm^{-1}. The values of the parameters g, D and E indicate the presence of magnetic anisotropy as expected for the tetrahedrally coordinated Co(II) atom.[34]

In summary we synthesized two isoreticular pillared-layer 2D CPs (**1** and **2**) of Co(II) with sdb and two linear bipyridyl spacer ligands with different lengths, bpy and bpe, forming polyrotaxane-type structures. The separation between the [Co$_2$(sdb)$_2$] layers has been varied due to the difference in lengths of the spacer ligands. Hence the variable temperature magnetic properties have been investigated for **1** and **2** which reflects the interplays between structural properties of samples and their magnetic behaviours.

Experimental

General

All chemicals were purchased from commercial sources and used as received. All solvents used were of reagent grade. Elemental analyses were carried out on a LECO CHNS-932 elemental analyzer. Thermogravimetric analyses were recorded in a TA Instruments TGA-Q50 thermogravimetric analyzer. Samples were heated at a constant rate of 5 °C min^{-1} from room temperature to 700 °C and at a continuous flow nitrogen atmosphere. The FT-IR spectra were recorded using Thermo Fisher Scientific Nicolet iS 10 FT-IR spectrometer with KBr pellets. Powder X-ray diffraction (PXRD) patterns were recorded usning Bruker D8 DISCOVER.

Preparation of [Co$_2$(bpy)(sdb)$_2$]·2H$_2$O (1)

A mixture of bpy (11.1 mg, 0.071 mmol), H$_2$sdb (22.1 mg, 0.072 mmol) and Co(NO$_3$)$_2$·6H$_2$O (21.0 mg, 0.072 mmol) dissolved in DMF (3 mL), H$_2$O (1 mL) and DMSO (0.5 mL) was placed in a 5 mL glass tube, and then 2–3 drops of 0.1 M NaOH solution was added. The tube was sealed and kept at 120 °C for 48 h, followed by cooling to room temperature over 8 h. Dark blue block-shaped crystals **1** suitable for single crystal X-ray diffraction (SC-XRD) analysis were obtained. Yield: 70%. Anal. calcd for [C$_{38}$H$_{27}$Co$_2$N$_2$O$_{13.5}$S$_2$]: C, 50.18; H, 2.99; N, 3.08; S, 7.05. Found: C, 50.15; H, 2.99; N, 3.20; S, 7.12%. IR (KBr pellet, cm^{-1}) 3432, 3093, 3061, 1629, 1568, 1490, 1409, 1326, 1301, 1217, 1169, 1138, 1101, 1071, 1015, 845, 812, 779, 723, 695, 618 and 584.

Preparation of [Co$_2$(bpe)(sdb)$_2$]·DMA·1.5H$_2$O (2)

A mixture of bpe (13.0 mg, 0.071 mmol), H$_2$sdb (21.9 mg, 0.071 mmol) and Co(NO$_3$)$_2$·6H$_2$O (20.8 mg, 0.071 mmol) dissolved in DMA (3 mL), H$_2$O (1 mL) and DMSO (0.5 mL) was placed in a 5 mL glass tube, and then 2–3 drops of 0.1 M NaOH solution was added. The tube was sealed and kept at 120 °C for 48 h, followed by cooling to room temperature over 8 h. Dark blue block-shaped crystals **2** suitable for SC-XRD analysis were obtained. Yield: 80%. Anal. calcd for [C$_{43}$H$_{35}$Co$_2$N$_3$O$_{14}$S$_2$]: C, 51.66; H, 3.53; N, 4.20; S, 6.41. Found: C, 51.82; H, 3.39; N, 4.27; S, 6.51%. IR (KBr pellet, cm^{-1}) 3401, 3095, 3044, 1635, 1612, 1569, 1490, 1409, 1328, 1301, 1169, 1138, 1101, 1070, 1029, 1016, 844, 779, 739, 696, 618 and 551.

Crystallographic structure determinations

Crystal data for **1** and **2** at 173 K were collected on a Bruker SMART APEX II ULTRA diffractometer equipped with graphite monochromated Mo Kα radiation ($\lambda = 0.71073$ Å) generated by a rotating anode. The cell parameters for the compounds were obtained from a least-squares refinement of the spot (from 36 collected frames). Data collection, data reduction and absorption correction were carried out using the software package of APEX2.[35] All of the calculations for the structure determination were carried out using the SHELXTL package.[36] Relevant crystal data collection and refinement data for the crystal structures of **1** and **2** are summarized in Table S1.† CCDC 1551657 (**1**) and 1551656 (**2**) contain the supplementary crystallographic data for this paper.†

Crystal 1. Hydrogen atoms on lattice water were not added. Although very high R-factors were observed, the connectivity in the 3D structure is proved beyond any doubt. Surprisingly the crystal structure of this paddlewheel based pillared-layer structure has higher crystallographic symmetry (*Cmcm* with $Z = 4$) than the simple paddlewheel structure observed in [Cu$_2$(OAc)$_4$(H$_2$O)$_2$] (*C2/c* with $Z = 4$).[37]

Crystal 2. One pyridyl group in bpe was disordered along the ligand axis and the occupancy was refined to 0.77(1). Further one disordered DMA and 1.5 disordered and scattered water molecules were found in the voids. Since the thermal parameters of the atoms of the DMA molecule was not satisfactory, we have resorted to SQUEEZE program. The final agreement factors were better and hence retained.

Magnetic studies

A superconducting quantum interference device (SQUID) magnetometer MPMS was used for the magnetic characterization. Powder sample with a weight of 5–10 mg was sealed in a plastic capsule. Magnetic moment was measured in the temperature range of 2 K to 350 K. The empty plastic capsule exhibited diamagnetism and its magnetic moment was measured for correction. After correction of diamagnetic signal of plastic capsule and sample holder, diamagnetism of

monomer and paramagnetic contamination (for example free radical), magnetic susceptibility was fitted using the PHI[31] program by means of an isotropic spin Hamiltonian (SH) accounting for the exchange coupling (Heisonberg–Dirac–van Vleck Hamitonian) and zero-field splitting (ZFC).

$$H = H_{ex} + H_{Zee} + H_{CF}$$

$$H_{ex} = -2J_{12}\vec{S}_1\vec{S}_2$$

$$H_{Zee} = \mu_B \sum_{i=1}^{2} \vec{S}_i g_i \vec{B}$$

$$H_{CF} = \sum D_i \left[S_{z,i}^2 - \frac{1}{3}S_i(S_i + 1) + \frac{E_i}{D_i}\left(S_{x,i}^2 - S_{y,i}^2\right) \right]$$

D: axial ZFS parameter; F: rhombic ZFS parameter; $\vec{S}$: spin vector; $\vec{B}$: magnetic field vector; g: g-factor; μ_B: Bohr magneton.

Conflicts of interest

There are no conflicts to declare.

Acknowledgements

References

1 S. R. Batten, S. M. Nevillle and D. R. Turner, *Coordination Polymers: Design, Analysis and Application*, RSC Publishing, London, 2009.

2 *Design and Construction of Coordination Polymers*, ed. M.-C. Hong and L. Chen, Wiley, 2009.

3 *Metal-Organic Frameworks: Design and Application*, ed. L. R. MacGillivray, Wiley, Weinheim, 2010.

4 *Functional Metal-Organic Frameworks: Gas Storage, Separation and Catalysis*, ed. M. Schröder, Topics in Current Chemistry, 2010, vol. 293.

5 *Metal-Organic Frameworks, Applications from Catalysis to Gas Storage*, ed. D. Farrusseng, Wiley-VCH, Weinheim, 2011.

6 *Metal Organic Frameworks as Heterogeneous Catalysts*, ed. F. L. i. Xamena and J. Gascon, RSC, 2013.

7 *Coordination Polymers and Metal Organic Frameworks: Properties, Types, and Applications (Chemical Engineering Methods and Technology)*, ed. O. L. Ortiz and L. D. Ramirez, Nova Science Publishers Inc, New York, 2012.

8 H. Ju, E. Lee, S. Kim, I.-H. Park, J.-H. Lee and S. S. Lee, *CrystEngComm*, 2016, **18**, 2621.

9 Y. Bu, F. Jiang, K. Zhou, Y. Gai and M. Hong, *CrystEngComm*, 2014, **16**, 1249.

10 J.-Q. Liu, J. Wu, Y.-Y. Wang, J.-Y. Lin and H. Skiyama, *CrystEngComm*, 2014, **16**, 3103.

11 J. Wu, J.-Q. Liu, Y.-Y. Wang, Z.-P. Gou, D.-H. Xu and H. Skiyama, *Inorg. Chem. Commun.*, 2012, **25**, 10.

12 J. Yang, J. F. Ma, S. R. Batten and Z. M. Su, *Chem. Commun.*, 2008, 2233.

13 H. Chen, D. Xiao, J. He, Z. Li, G. Zhang, D. Sun, R. Yuan, E. Wang and Q.-L. Luo, *CrystEngComm*, 2011, **13**, 4988.

14 H. Wu, H. Y. Liu, B. Liu, J. Yang, Y. Y. Liu, J. F. Ma, Y. Y. Liu and H. Y. Bai, *CrystEngComm*, 2011, **13**, 3402.

15 F. Luo, Y. T. Yang, Y. X. Che and J. M. Zheng, *CrystEngComm*, 2008, **10**, 981.

16 Y. Q. Lan, S. L. Li, J. S. Qin, D. Y. Du, X. L. Wang, Z. M. Su and Q. Fu, *Inorg. Chem.*, 2008, **47**, 10600.

17 S. R. Batten, *CrystEngComm*, 2001, **18**, 1.

18 S. R. Batten and R. Robson, *Angew. Chem., Int. Ed.*, 1998, **37**, 1460.

19 X. Guo, Y. Yan, H. Guo, Y. Qi and C. Liu, *CrystEngComm*, 2016, **18**, 2546.

20 M.-D. Zhang, B.-H. Zheng, L. Chen, M.-D. Chen, T. Tao, K. Chen and H. Cao, *Dalton Trans.*, 2016, **45**, 3334.

21 L.-L. Liu, C.-X. Yu, F.-J. Ma, Y.-R. Li, J.-J. Han, L. Lin and L.-F. Ma, *Dalton Trans.*, 2015, **44**, 1636.

22 Y. Li, X.-Q. Yao, G.-B. Xiao, H.-C. Ma, Y.-X. Yang and J.-C. Liu, *J. Mol. Struct.*, 2015, **1089**, 16.

23 S.-L. Wang, F.-L. Hu, J.-Y. Zhou, Y. Zhou, Q. Huang and J.-P. Lang, *Cryst. Growth Des.*, 2015, **15**, 4087.

24 H.-D. Guo, Z.-A. Fu, X.-M. Guo, X.-L. Li, R.-Z. Chen, Y.-J. Qi and H.-Y. Zou, *J. Mol. Struct.*, 2013, **1038**, 8.

25 Y. Ma, A.-L. Cheng and E.-Q. Gao, *Cryst. Growth Des.*, 2010, **10**, 2832.

26 I.-H. Park, R. Medishetty, J.-Y. Kim, S. S. Lee and J. J. Vittal, *Angew. Chem., Int. Ed.*, 2014, **53**, 5591.

27 I.-H. Park, H. Ju, T. S. Herng, Y. Kang, S. S. Lee, J. Ding and J. J. Vittal, *Cryst. Growth Des.*, 2016, **16**, 7278.

28 A. L. Spek, *J. Appl. Crystallogr.*, 2003, **36**, 7.

29 A. L. Spek, *Acta Crystallogr., Sect. D: Biol. Crystallogr.*, 2009, **65**, 148.

30 P. van der Sluis and A. L. Spek, *Acta Crystallogr., Sect. A: Found. Crystallogr.*, 1990, **46**, 194.

31 N. F. Chilton, R. P. Anderson, L. D. Turner, A. Soncini and K. S. Murray, *J. Comput. Chem.*, 2013, **34**, 1164.

32 L. Qin, J.-S. Hu, L.-F. Huang, Y.-Z. Li, Z.-J. Guo and H.-G. Zheng, *Cryst. Growth Des.*, 2010, **10**, 4176.

33 N. Benbellat, K. S. Gavrilenko, Y. L. Gal, O. Cador, S. Golhen, A. Gouasmia, J.-M. Fabre and L. Ouahab, *Inorg. Chem.*, 2006, **45**, 10440.

34 R. Boča, *Coord. Chem. Rev.*, 2004, **248**, 757.

35 Bruker, *APEX2 Version 2009.1-0 Data Collection and Processing Software*, Bruker AXS Inc., Madison, Wisconsin, U.S.A., 2008.

36 Bruker, *SHELXTL-PC Version 6.22 Program for Solution and Refinement of Crystal Structures*, Bruker AXS Inc., Madison, Wisconsin, U.S.A, 2001.

37 P. de Meester, S. R. Fletcher and A. C. Skapski, *J. Chem. Soc., Dalton Trans.*, 1973, 2575.